

PAPER

Single-photon-added coherent states: estimation of parameters and fidelity of the optical homodyne detection

To cite this article: S N Filippov *et al* 2013 *Phys. Scr.* **2013** 014025

View the [article online](#) for updates and enhancements.

You may also like

- [Deformed photon-added entangled squeezed vacuum and one-photon states: Entanglement, polarization, and nonclassical properties](#)
A Karimi and M K Tavassoly
- [Phase Properties of Photon-Added Coherent States for Nonharmonic Oscillators in a Nonlinear Kerr Medium](#)
F. Jahanbakhsh and G. Honarasa
- [Complementarity, quartic polynomials and one-photon-added coherent and squeezed states](#)
Ramón F Álvarez-Estrada

Single-photon-added coherent states: estimation of parameters and fidelity of the optical homodyne detection

S N Filippov^{1,2}, V I Man'ko^{1,3}, A S Coelho⁴, A Zavatta^{5,6} and M Bellini^{5,6}

¹ Moscow Institute of Physics and Technology, 141700 Moscow Region, Russia

² Institute of Physics and Technology, Russian Academy of Sciences, 117218 Moscow, Russia

³ P N Lebedev Physical Institute, Russian Academy of Sciences, 119991 Moscow, Russia

⁴ Instituto de Física, Universidade de São Paulo, 05315-970 São Paulo, Brazil

⁵ Istituto Nazionale di Ottica, INO-CNR, Largo Enrico Fermi 6, I-50125 Florence, Italy

⁶ LENS, Via Nello Carrara 1, I-50019 Sesto Fiorentino, Florence, Italy

E-mail: sergey.filippov@phystech.edu

Received 1 November 2012

Accepted for publication 3 December 2012

Published 28 March 2013

Online at stacks.iop.org/PhysScr/T153/014025

Abstract

The travelling modes of single-photon-added coherent states (SPACS) are characterized by using optical homodyne tomography. Given a set of experimentally measured quadrature distributions, we estimate parameters of the state and also extract information about the detector efficiency. The method used is minimal distance estimation between theoretical and experimental quantities, which additionally allows to evaluate the precision of the estimated parameters. Given the experimental data, we also estimate the lower and upper bounds on fidelity. The results are believed to encourage a more precise engineering and detection of SPACS.

PACS numbers: 03.65.Ta, 03.65.Wj, 42.50.Xa, 42.50.Dv

(Some figures may appear in colour only in the online journal)

1. Introduction

Optical homodyne tomography is a powerful technique to infer continuous-variable quantum states of a specific mode of electromagnetic radiation. Its history saw a dramatic boom in the last two decades, when both theoretical and experimental methods evolved significantly from the first proof-of-principle studies [1–3] to the state-of-the-art detection of arbitrarily shaped ultrashort quantum light states [4] and the experimental analysis of decoherence in continuous-variable bipartite systems [5]. Different stages of the research in this area can be seen in the monographs and reviews [6–11], where different approaches to the state reconstruction are outlined and corresponding experimental realizations are discussed.

The goal of this paper is to consider both theoretically and experimentally the detection of single-photon-added coherent states (SPACS). These states are defined by the formula $a^\dagger|\alpha\rangle/\sqrt{1+|\alpha|^2}$, where $|\alpha\rangle$ is a conventional coherent state

$(\alpha \in \mathbb{C})$ and a^\dagger is a photon creation operator. Photon-added states of light and their non-classical properties were considered originally in the papers [12, 13] and then realized in practice [14, 15]. The techniques of photon addition and subtraction allowed to check experimentally the commutation relation between the corresponding operators [16–18]. The process tomography of photon creation and annihilation operators was recently reported [19]. The nonclassical behaviour of photon-added states was demonstrated in the papers [20–22] and noiseless amplification was discussed in [23].

The practical homodyne detection of some signals results in experimental quadrature distributions $w_{\text{ex}}(X, \theta)$ to be compared with the theoretically predicted ones $w_{\text{th}}(X, \theta)$. An adequate theoretical model should take losses into account, which are usually modelled by fictitious beamsplitters with transmittivity η placed in front of ideal detectors. In the paper [15], the explicit form of such theoretical quadrature distributions $w_{\text{th}}(X, \theta)$ for SPACS is found for any η . We can

associate density operators ρ_{ex} and ρ_{th} with distributions $w_{\text{ex}}(X, \theta)$ and $w_{\text{th}}(X, \theta)$, respectively. Note that these states are mixed in general and depend on the parameters α and η .

We can naturally define the fidelity of detection as the fidelity between ρ_{ex} and ρ_{th} , i.e. $F = \text{Tr}[\sqrt{\rho_{\text{ex}}}\sqrt{\rho_{\text{th}}}] \equiv \text{Tr}\sqrt{\sqrt{\rho_{\text{th}}}\rho_{\text{ex}}\sqrt{\rho_{\text{th}}}}$. It is tempting to express F directly through the measured distributions $w_{\text{ex}}(X, \theta)$ avoiding reconstruction of the state ρ_{ex} and dealing with complicated formulae. The easiest way is to find the Bhattacharyya coefficient [24] for distributions $w_{\text{ex}}(X, \theta)$ and $w_{\text{th}}(X, \theta)$, which turns out to be the upper bound for F [25]. Alternatively, one can use the upper and lower bounds for F^2 that were developed in the paper [26] and are also known as super- and sub-fidelity, respectively. In this paper, we present operational ways to calculate these quantities.

In principle, maximizing the sub-fidelity with respect to α and η would enable us to estimate both these parameters. As will be shown by an example in section 4, such a method can be applied to extremely precise data only. If this is not the case, parameters α and η can be estimated by minimizing another distance between the states ρ_{ex} and ρ_{th} (not the Bures distance related to the fidelity). Fortunately, the Hilbert–Schmidt distance is easy to compute via tomograms and its minimization is performed in section 3. As a result, an operational estimation of state and measurement parameters is achieved. Finally, errors of the estimated parameters are evaluated by using the symmetry condition $w(X, \theta + \pi) = w(-X, \theta)$ met by fair optical tomograms. This approach was suggested and demonstrated in the papers [27] and [28], respectively. The improved precision of homodyne detection is of vital importance to check different uncertainty relations (see [28] and references therein) as well as to probe commutation relations between position and momentum of massive particles, which may be modified by gravity and feasibly detected with the help of quantum optics [29].

The paper is organized as follows. In section 2, we recall the explicit formula of homodyne quadrature distributions of SPACS modified by the losses. In section 3, we present theoretical basics and demonstrate particular results of the minimal distance estimation of the state and apparatus parameters. In section 4, the fidelity of detection is discussed. In section 5, we briefly summarize the results obtained and outline the prospects.

2. Quadrature distributions of SPACS

Generation of SPACS is due to injection of a coherent state $|\alpha\rangle$ into the signal mode of an optical parametric amplifier. The stimulated emission of a single down-converted photon into the signal mode results in SPACS generation, which is triggered by the detection of a single photon in the idler mode of the amplifier. A time-domain balanced homodyne detector is then used to acquire quadrature data (see, e.g., the review [8]).

The balanced homodyne detection is known to give access to quadratures $\hat{X}_\theta = \hat{Q} \cos \theta + \hat{P} \sin \theta$, where $[\hat{Q}, \hat{P}] = i$ and $\theta \in [0, 2\pi]$ is a phase of an intense coherent light (the local oscillator). Once θ is fixed, the distribution of quadratures is given by the optical tomogram

$w_{\text{th}}(X, \theta) = \langle X_\theta | \rho | X_\theta \rangle$, where ρ is the density operator of the quantum state and $\hat{X}_\theta | X_\theta \rangle = X | X_\theta \rangle$.

Let ρ be a density operator of SPACS; then the tomogram $\tilde{w}_{\text{th}}(X, \theta) = \langle X_\theta | \rho | X_\theta \rangle$ is easy to compute. However, it turns out that the experimentally measured quadrature distributions are smoother than the predicted ones and can differ significantly from them. This takes place due to losses and overall efficiency of detection $\eta < 1$. One can make allowance for losses by introducing a fictitious beamsplitter with transmittivity η in front of the ideal photodetectors (with a sensitivity of 100%). Such an attenuation of the signal results in the following convolution relation between the quadrature distributions [30]:

$$w_{\text{th}}(X, \theta; \eta) = \frac{1}{\sqrt{\pi(1-\eta)}} \int \tilde{w}_{\text{th}}(Y, \theta) \times \exp \left[-\frac{\eta}{1-\eta} (Y - \sqrt{\eta}X)^2 \right] dY. \quad (1)$$

In the Schrödinger picture, the distribution $w_{\text{th}}(X, \theta; \eta)$ is nothing else but the optical tomogram $\langle X_\theta | \mathcal{E}_\eta[\rho] | X_\theta \rangle$ of the transformed state $\mathcal{E}_\eta[\rho]$, where $\mathcal{E}_\eta[\bullet] = \sum_{k=0}^{\infty} A_k(\eta) \bullet A_k^\dagger(\eta)$ is a completely positive trace preserving map with the following operator-sum representation: $A_k(\eta) = \sum_{m=0}^{\infty} \sqrt{\frac{(m+k)!}{m!k!}} \eta^m (1-\eta)^k |m\rangle \langle m+k|$ (see, e.g., [6, 31]).

Using formula (1), one can calculate in an explicit form the optical homodyne tomogram of a SPACS. Some algebra yields

$$w_{\text{th}}(X, \theta; \alpha, \eta) = \frac{1}{\sqrt{\pi(1+|\alpha|^2)}} \left\{ (1-\eta)(1+4\eta|\alpha|^2 \sin^2(\theta-\varphi)) + 2\eta \left[\left(X \cos(\theta-\varphi) - \frac{2\eta-1}{\sqrt{2\eta}} |\alpha| \right)^2 + X^2 \sin^2(\theta-\varphi) \right] \right\} \times \exp \left[- \left(X - \sqrt{2\eta} |\alpha| \cos(\theta-\varphi) \right)^2 \right]. \quad (2)$$

An analogue of tomogram (2) was first derived in the paper [15], where the authors used a slightly different commutation relation $[\hat{Q}, \hat{P}] = \frac{i}{2}$. The deduced tomogram (2) comprises two parameters: $\alpha = |\alpha| e^{i\varphi}$ determines the coherent state $|\alpha\rangle$ to which a single photon is added, and η is the overall efficiency of homodyne detection and characterizes the imperfection of the measurement device. The overall efficiency includes transmission losses, mode matching and the intrinsic quantum efficiency of detectors.

3. Estimation of parameters

Our goal is to compare $w_{\text{th}}(X, \theta; \alpha, \eta)$ with the experimentally measured distributions $w_{\text{ex}}(X, \theta)$ and find parameters $\alpha = |\alpha| e^{i\varphi}$ and η resulting in the best fitting. In this sense, we perform a minimal distance estimation of the state parameter α and the detector parameter η . In order to give this procedure a more rigorous formulation with clearer physical meaning, we need to choose such a distance between distributions $w_{\text{th}}(X, \theta; \alpha, \eta)$ and $w_{\text{ex}}(X, \theta)$ that is related to some fair distance between states $\rho_{\text{th}} \equiv \mathcal{E}_\eta[\rho]$ and ρ_{ex} (satisfying metric requirements). Moreover, we are

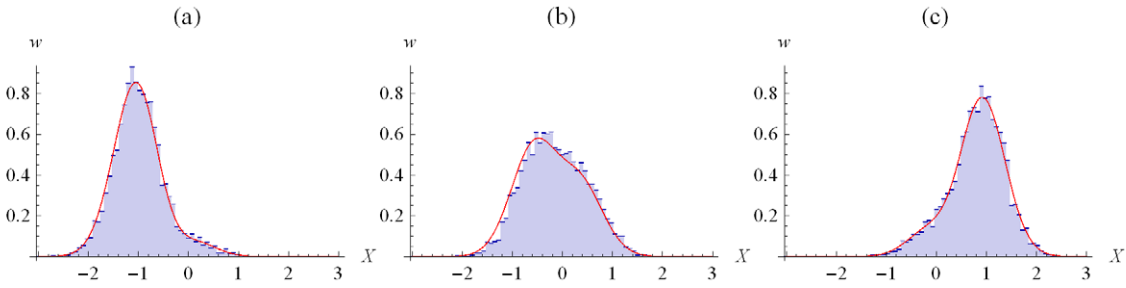


Figure 1. Experimental histograms $w_{\text{ex}}(X, \theta)$ (blue discontinuous lines) and the closest theoretical quadrature distributions $w_{\text{th}}(X, \theta)$ (red solid lines) of a SPACS for different phases: $\theta = 0$ (a), $\theta = 1.36$ (b) and $\theta = 2.49$ (c).

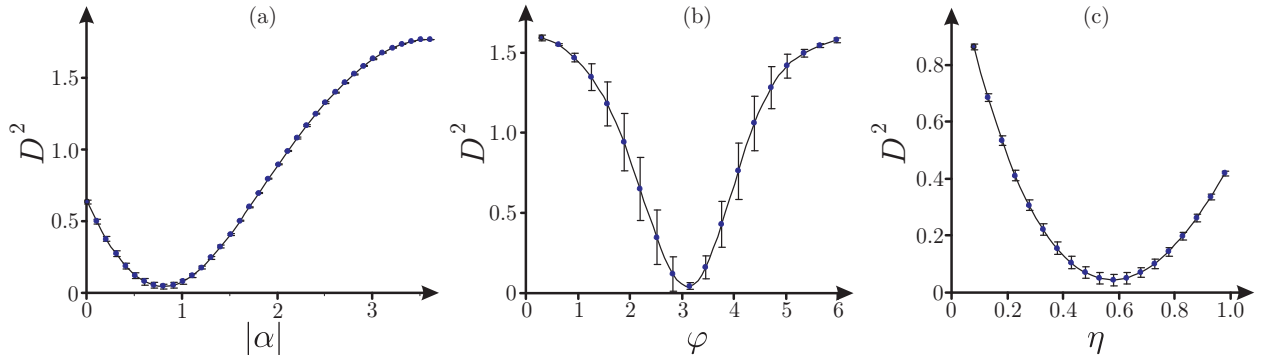


Figure 2. Square of the Hilbert–Schmidt distance versus state and detector parameters in the vicinity of the global minimum: $D^2(|\alpha|, \varphi_{\text{opt}}, \eta_{\text{opt}})$ (a), $D^2(|\alpha|_{\text{opt}}, \varphi, \eta_{\text{opt}})$ (b) and $D^2(|\alpha|_{\text{opt}}, \varphi_{\text{opt}}, \eta)$ (c).

interested in such a distance between the states that could be operationally calculated via optical tomograms. Some aspects of appropriate distances are discussed in the paper [32]. The Hilbert–Schmidt distance $D = \sqrt{\text{Tr}(\rho_{\text{th}} - \rho_{\text{ex}})^2}$ turns out to be suitable because it can be given by the following expression in terms of tomograms:

$$D^2(\alpha, \eta) = \frac{1}{\pi} \int_0^{+\infty} dr r \iint_{-\infty}^{+\infty} dX dY \cos[(X + Y)r] \times \int_0^{\pi} d\theta [w_{\text{ex}}(X, \theta) - w_{\text{th}}(X, \theta; \alpha, \eta)] \times [w_{\text{ex}}(-Y, \theta) - w_{\text{th}}(-Y, \theta; \alpha, \eta)], \quad (3)$$

which can be readily deduced with the help of a formula for $\text{Tr}\rho_1\rho_2$ obtained in [33]. Similarly, the experimental error is evaluated by a slight modification of the formulae in the paper [28], namely

$$\Delta(D^2) = \frac{1}{2\pi} \int_0^{+\infty} dr r \iint_{-\infty}^{+\infty} dX dY \cos[(X + Y)r] \times \int_0^{\pi} d\theta [w_{\text{ex}}(X, \theta)w_{\text{ex}}(-Y, \theta) - w_{\text{ex}}(X, \theta + \pi) \times w_{\text{ex}}(-Y, \theta + \pi) + 2w_{\text{th}}(X, \theta)(w_{\text{ex}}(Y, \theta + \pi) - w_{\text{ex}}(-Y, \theta))]. \quad (4)$$

Formula (4) is based on the fact that the fair quadrature distributions satisfy the symmetry relation $w(X, \theta + \pi) = w(-X, \theta)$. Experimentally measured distributions do not satisfy precisely this relation, and this gives rise to the error (4) which includes both systematic and statistical components (for details see the paper [28]).

3.1. Results

In this subsection, we estimate parameters $|\alpha|$, φ and η for a particular set of experimental quadrature distributions. Phases of the local oscillator take discrete values $\{\theta_j\}_{j=1}^{21}$. For each fixed phase, the quadrature distribution is a histogram of 5321 values, with the bin width being chosen to guarantee the statistical confidence and prevent the data from undersampling [28]. Examples of experimental histograms are depicted in figure 1. Thus, the data are presented in discrete form so the integrals in formulae (3) and (4) are calculated approximately by the trapezoid method [35]. The error of calculation is estimated in the paper [28] and is usually less than the experimental quantity (4).

In our particular case, the minimization of the square of distance $D^2(|\alpha|, \varphi, \eta)$ results in $D^2 = 0.0436$, which is achieved at $|\alpha|_{\text{opt}} = 0.81$, $\varphi_{\text{opt}} = 3.14$, $\eta_{\text{opt}} = 0.58$. On substituting these parameters in formula (2), we can depict the closest theoretical quadrature distributions (see figure 1).

In order to evaluate the errors of estimated parameters $|\alpha|_{\text{opt}}$, φ_{opt} , and η_{opt} we consider three cuts of the function $D^2(|\alpha|, \varphi, \eta)$ that cross at the point $(|\alpha|_{\text{opt}}, \varphi_{\text{opt}}, \eta_{\text{opt}})$. The values of the function and their errors are shown in figure 2. Further, the error of an optimal parameter q_{opt} can be evaluated as $\Delta q/\text{SNR}$, where Δq is the width of the corresponding function cut and $\text{SNR} = (\max D^2 - \min D^2)/\max \Delta(D^2)$ plays the role of the signal-to-noise ratio. The errors evaluated in such a way give rise to the following results: $|\alpha|_{\text{opt}} = 0.81 \pm 0.03$, $\varphi_{\text{opt}} = 3.14 \pm 0.25$, $\eta_{\text{opt}} = 0.58 \pm 0.02$. The least precise parameter is the phase φ and this can be attributed to the relatively small mean number of photons $\langle n \rangle \lesssim 1$ and imprecise fixing of the local oscillator phase θ . Improving control of this parameter would result in higher precision of parameters under estimation.

4. Fidelity of detection

Sometimes, the Hilbert–Schmidt distance between the states is not very representative because it can grow under the action of quantum operations (not monotone metric). In this case one exploits some other quantities, e.g. the Bures distance $D_B = \sqrt{2(1-F)}$, where $F = \text{Tr} \sqrt{\sqrt{\rho_{\text{th}}} \rho_{\text{ex}} \sqrt{\rho_{\text{th}}}}$ is Uhlmann’s fidelity (see, e.g., the book [36]). The fidelity is difficult to express in an operational way through quadrature distributions. Nevertheless, we can use recently found bounds for fidelity: the sub-fidelity E and the super-fidelity G that were satisfying $E \leq F^2 \leq G$ and given by the formulae [26, 37, 38]

$$E(\rho_{\text{th}}, \rho_{\text{ex}}) = \text{Tr} \rho_{\text{th}} \rho_{\text{ex}} + \sqrt{2[(\text{Tr} \rho_{\text{th}} \rho_{\text{ex}})^2 - \text{Tr} \rho_{\text{th}} \rho_{\text{ex}} \rho_{\text{th}} \rho_{\text{ex}}]}, \quad (5)$$

$$G(\rho_{\text{th}}, \rho_{\text{ex}}) = \text{Tr} \rho_{\text{th}} \rho_{\text{ex}} + \sqrt{(1 - \text{Tr} \rho_{\text{th}}^2)(1 - \text{Tr} \rho_{\text{ex}}^2)}. \quad (6)$$

The overlap $\text{Tr} \rho_{\text{th}} \rho_{\text{ex}}$ and purity $\text{Tr} \rho_{\text{ex}}^2$ are readily expressed through tomograms (see, e.g., [33]). It is worth noting that the purity can also be estimated by exploiting the covariant uncertainty relation [34]. As far as four-product $\text{Tr} \rho_{\text{th}} \rho_{\text{ex}} \rho_{\text{th}} \rho_{\text{ex}}$ is concerned, we can approximate it by $\text{Tr} \rho_{\text{th}}^4$. In fact, we have $|\text{Tr} \rho_{\text{th}} \rho_{\text{ex}} \rho_{\text{th}} \rho_{\text{ex}} - \text{Tr} \rho_{\text{th}}^4| \leq |\text{Tr} \rho_{\text{ex}} \rho_{\text{th}} \rho_{\text{ex}} - \text{Tr} \rho_{\text{th}}^3| \leq |\text{Tr} \rho_{\text{ex}}^2 - \text{Tr} \rho_{\text{th}}^2|$ and can modify the sub-fidelity as follows:

$$E'(\rho_{\text{th}}, \rho_{\text{ex}}) = \text{Tr} \rho_{\text{th}} \rho_{\text{ex}} + \sqrt{2[(\text{Tr} \rho_{\text{th}} \rho_{\text{ex}})^2 - \text{Tr} \rho_{\text{th}}^4 - |\text{Tr} \rho_{\text{ex}}^2 - \text{Tr} \rho_{\text{th}}^2|]}. \quad (7)$$

In order to be able to calculate the modified sub-fidelity (7) for SPACS, we find the following theoretical values:

$$\text{Tr} \rho_{\text{th}}^2 = 1 - \frac{2\eta(1-\eta)}{(1+|\alpha|^2)^2}, \quad (8)$$

$$\text{Tr} \rho_{\text{th}}^4 = 1 - \frac{4\eta(1-\eta)}{(1+|\alpha|^2)^2} + \frac{2\eta^2(1-\eta)^2}{(1+|\alpha|^2)^4}. \quad (9)$$

Returning to the example considered earlier, we substitute the experimental data and the optimal theoretical values $|\alpha|_{\text{opt}} = 0.81$, $\varphi_{\text{opt}} = 3.14$, $\eta_{\text{opt}} = 0.58$ into formula (6) and obtain the upper bound $G(\rho_{\text{th}}, \rho_{\text{ex}}) = 0.98 \pm 0.02$. In our case, the direct calculation of sub-fidelity (7) turns out to be problematic because the confidence interval of the radicand is $[-0.07; 0.05]$ (cf $2[(\text{Tr} \rho_{\text{th}}^2)^2 - \text{Tr} \rho_{\text{th}}^4] = 0.032$). Thus, the calculation of square root is worthless. Therefore, the use of formula (7) is possible only with the data of very high precision (errors should be substantially less than 1%). Whenever this does not happen, one can use another lower bound $E'' = \text{Tr} \rho_{\text{th}} \rho_{\text{ex}} \leq F^2$ (see, e.g., [26]). This lower bound is easy to calculate and in our case it equals $E'' = 0.81 \pm 0.02$. Consequently, the fidelity of our interest is bounded by the two-sided inequality $0.81 \pm 0.02 \leq F^2 \leq 0.98 \pm 0.02$.

5. Conclusions

In order to estimate parameters of some prepared SPACS, we developed the operational method whose essence was the comparison of experimental histograms with theoretically predicted quadrature distributions. The explicit form of theoretical distributions took into account the losses presented, which allowed us to infer not only the state parameter α but also the parameter η describing the overall efficiency of homodyne detection. We discussed some practical issues concerning the easiest way to calculate the Hilbert–Schmidt distance and evaluate the errors of estimated parameters. The phase of the state turned out to be the least precise parameter, which could be ascribed to the small intensity of the signal mode and the errors in control of the local oscillator phase. Then we considered some operational techniques to determine the lower and upper bounds for fidelity of detection. We showed that, in practice, some of these bounds can be calculated only with highly precise data.

The outlook for further research is to use the high sensitivity of homodyne detection to trace all the stages of the quantum state’s life: its preparation, transformation via a quantum channel, and detection. Using appropriate theoretical models of these processes, one can determine the corresponding parameters. For instance, dark counts in the trigger detector result in mixing of the SPACS with a residual coherent state. In this case, the measured tomogram reads $(1-p)w_{\text{SPACS}} + p w_{\text{coherent}}$, where p is a fraction of dark counts. The parameter p can be estimated by the same algorithm of comparing w_{ex} and w_{th} .

In general, optical tomograms can be valuable information sources on an equal footing with other state descriptions [39]. Improving the accuracy of homodyne detection, one can check the validity of more complicated quantum theories and observe new phenomena (see, e.g., [29]). The role of SPACS states for new experiments can be also dramatic because of their ability to exhibit properties ranging from classical to quantum ones for different intensities [14].

Acknowledgments

SNF and VIM are grateful to the organizers of the 19th Central European Workshop on Quantum Optics (Sinaia, Romania, 2–6, July 2012) for the invitation and kind hospitality. SNF would like to express his gratitude to the organizing committee of the conference and especially to Dr Aurelian Isar for financial support. SNF and VIM thank the Russian Foundation for Basic Research for partial support under project numbers 10-02-00312-a and 11-02-00456-a and the Ministry of Education and Science of the Russian Federation for partial support under project number 2.1759.2011. SNF also acknowledges support from the Russian Foundation for Basic Research under project number 12-02-31524-mol-a and the Dynasty Foundation (www.dynastyfdn.com). ASC acknowledges financial support from the Fundação de Amparo à Pesquisa do Estado São Paulo (FAPESP). AZ and MB acknowledge support from Ente Cassa di Risparmio di Firenze, Regione Toscana under the project CTOTUS, the EU under the ERA-NET CHIST-ERA project QSCALE, and the MIUR under the contract FIRB RBFR10M3SB.

References

[1] Vogel K and Risken H 1989 *Phys. Rev. A* **40** 2847

[2] Smithey D T, Beck M, Raymer M G and Faridani A 1993 *Phys. Rev. Lett.* **70** 1244

[3] Schiller S, Breitenbach G, Pereira S F, Müller T and Mlynek J 1996 *Phys. Rev. Lett.* **77** 2933

[4] Polycarpou C, Cassemiro K N, Venturi G, Zavatta A and Bellini M 2012 *Phys. Rev. Lett.* **109** 053602

[5] Buono D, Nocerino G, Porzio A and Solimeno S 2012 *Phys. Rev. A* **86** 042308

[6] Leonhardt U 1997 *Measuring the Quantum State of Light* (Cambridge: Cambridge University Press)

[7] Bachor H-A and Ralph T C 2004 *A Guide to Experiments in Quantum Optics* 2nd edn (Weinheim: Wiley-VCH) section 8

[8] Zavatta A, Viciani S and Bellini M 2006 *Laser Phys. Lett.* **3** 3

[9] Vogel W and Welsch D-G 2006 *Quantum Optics* 3rd revised and extended edn (Weinheim: Wiley-VCH) sections 6 and 7

[10] Walls D F and Milburn G J 2008 *Quantum Optics* 2nd edn (Berlin: Springer)

[11] Lvovsky A I and Raymer M G 2009 *Rev. Mod. Phys.* **81** 299

[12] Agarwal G S and Tara K 1991 *Phys. Rev. A* **43** 492

[13] Dodonov V V, Marchiolli M A, Korennoy Ya A, Man'ko V I and Moukhin Y A 1998 *Phys. Rev. A* **58** 4087

[14] Zavatta A, Viciani S and Bellini M 2004 *Science* **306** 660

[15] Zavatta A, Viciani S and Bellini M 2005 *Phys. Rev. A* **72** 023820

[16] Parigi V, Zavatta A, Kim M and Bellini M 2007 *Science* **317** 1890

[17] Kim M S, Jeong H, Zavatta A, Parigi V and Bellini M 2008 *Phys. Rev. Lett.* **101** 260401

[18] Zavatta A, Parigi V, Kim M S, Jeong H and Bellini M 2009 *Phys. Rev. Lett.* **103** 140406

[19] Kumar R, Barrios E, Kupchak C and Lvovsky A I 2012 Experimental characterization of bosonic photon creation and annihilation operators arXiv:1210.1150v1 [quant-ph]

[20] Zavatta A, Parigi V and Bellini M 2007 *Phys. Rev. A* **75** 052106

[21] Parigi V, Zavatta A and Bellini M 2009 *J. Phys. B: At. Mol. Opt. Phys.* **42** 114005

[22] Kiesel T, Vogel W, Bellini M and Zavatta A 2011 *Phys. Rev. A* **83** 032116

[23] Zavatta A, Fiurášek J and Bellini M 2011 *Nature Photon.* **5** 52

[24] Bhattacharyya A 1943 *Bull. Calcutta Math. Soc.* **35** 99

[25] Filippov S N and Man'ko V I 2010 *Phys. Scr.* **T140** 014043

[26] Miszczak J A, Puchała Z, Horodecki P, Uhlmann A and Życzkowski K 2009 *Quantum Inform. Comput.* **9** 0103

[27] Filippov S N and Man'ko V I 2011 *Phys. Scr.* **83** 058101

[28] Bellini M, Coelho A S, Filippov S N, Man'ko V I and Zavatta A 2012 *Phys. Rev. A* **85** 052129

[29] Pikovski I, Vanner M R, Aspelmeyer M, Kim M S and Brukner Č 2012 *Nature Phys.* **8** 393

[30] Leonhardt U and Paul H 1993 *Phys. Rev. A* **48** 4598

[31] Ivan J S, Sabapathy K K and Simon R 2011 *Phys. Rev. A* **84** 042311

[32] Dodonov V V, Man'ko O V, Man'ko V I and Wünsche A 1999 *Phys. Scr.* **59** 81

[33] Man'ko M A and Man'ko V I 2011 *AIP Conf. Proc.* **1334** 217

[34] Man'ko V I, Marmo G, Porzio A, Solimeno S and Ventriglia F 2011 *Phys. Scr.* **83** 045001

[35] Korn G A and Korn T M 1968 *Mathematical Handbook for Scientists and Engineers: Definitions, Theorems and Formulas for Reference and Review* 2nd enlarged and revised edn (New York: McGraw-Hill) section 20.7-2

[36] Bengtsson I and Życzkowski K 2006 *Geometry of Quantum States* (New York: Cambridge University Press) section 13.3

[37] Chen J-L, Fu L, Ungar A A and Zhao X-G 2002 *Phys. Rev. A* **65** 054304

[38] Mendonça P E M F, Napolitano R d J, Marchiolli M A, Foster C J and Liang Y-C 2008 *Phys. Rev. A* **78** 052330

[39] Ibort A, Man'ko V I, Marmo G, Simoni A and Ventriglia F 2009 *Phys. Scr.* **79** 065013